Journal of Experimental Botany, Vol. 66, No. 15 pp. 4497–4510, 2015
doi:10.1093/jxb/erv216 Advance Access publication 8 May 2015
This paper is available online free of all access charges (see http://jxb.oxfordjournals.org/open_access.html for further details)

RESEARCH PAPER

Comparative proteomics of root plasma membrane proteins reveals the involvement of calcium signalling in NaCl-facilitated nitrate uptake in *Salicornia europaea*

Lingling Nie[1,*], Juanjuan Feng[1,*], Pengxiang Fan[1,2,*], Xianyang Chen[1], Jie Guo[1], Sulian Lv[1], Hexigeduleng Bao[1,3], Weitao Jia[1], Fang Tai[1], Ping Jiang[1], Jinhui Wang[1] and Yinxin Li[1,†]

[1] Key Laboratory of Plant Molecular Physiology, Institute of Botany, Chinese Academy of Sciences, Beijing 100093, PR China
[2] Department of Biochemistry and Molecular Biology, Michigan State University, 603 Wilson Road, East Lansing, MI 48824, USA
[3] Shanghai Center for Plant Stress Biology (PSC), Chinese Academy of Sciences, No. 3888 Chenhua Road, Songjiang District, Shanghai 201602, PR China

* These authors contributed equally to this work.
† To whom correspondence should be addressed. E-mail: yxli@ibcas.ac.cn

Received 8 January 2015; Revised 31 March 2015; Accepted 8 April 2015

Editor: Timothy Colmer

Abstract

Improving crop nitrogen (N) use efficiency under salinity is essential for the development of sustainable agriculture in marginal lands. *Salicornia europaea* is a succulent euhalophyte that can survive under high salinity and N-deficient habitat conditions, implying that a special N assimilation mechanism may exist in this plant. In this study, phenotypic and physiological changes of *S. europaea* were investigated under different nitrate and NaCl levels. The results showed that NaCl had a synergetic effect with nitrate on the growth of *S. europaea.* In addition, the shoot nitrate concentration and nitrate uptake rate of *S. europaea* were increased by NaCl treatment under both low N and high N conditions, suggesting that nitrate uptake in *S. europaea* was NaCl facilitated. Comparative proteomic analysis of root plasma membrane (PM) proteins revealed 81 proteins, whose abundance changed significantly in response to NaCl and nitrate. These proteins are involved in metabolism, cell signalling, transport, protein folding, membrane trafficking, and cell structure. Among them, eight proteins were calcium signalling components, and the accumulation of seven of the above-mentioned proteins was significantly elevated by NaCl treatment. Furthermore, cytosolic Ca^{2+} concentration ($[Ca^{2+}]_{cyt}$) was significantly elevated in *S. europaea* under NaCl treatment. The application of the Ca^{2+} channel blocker $LaCl_3$ not only caused a decrease in nitrate uptake rate, but also attenuated the promoting effects of NaCl on nitrate uptake rates. Based on these results, a possible regulatory network of NaCl-facilitated nitrate uptake in *S. europaea* focusing on the involvement of Ca^{2+} signalling was proposed.

Key words: $[Ca^{2+}]_{cyt}$, calcium signalling, 2D-DIGE, NaCl, nitrate uptake, plasma membrane, *Salicornia europaea.*

Introduction

Salinity is among the most severe abiotic stresses in agriculture that affects ~6% of the total land on earth (Munns and Tester, 2008). In saline soil, the salt concentration is high, whereas the nitrogen (N) content is usually deficient (Hamed *et al.*, 2013); most crops could not survive on it. However, many halophytes can thrive in this type of infertile soil,

Abbreviations: ANN, annexin; ANOVA, analysis of variance; $[Ca^{2+}]_{cyt}$, cytosolic Ca^{2+} concentration; CaM, calmodulin; CBL, calcineurin B-like; CDPK, calcium-dependent protein kinase; CIPK, calcium-independent protein kinase; CML, calmodulin-like; CRT, calreticulin; 2D-DIGE, two-dimensional fluorescence difference gel electrophoresis; DW, dry weight; FW, fresh weight; GDH, glutamate dehydrogenase; GS, glutamine synthase; NiR, nitrite reductase; NR, nitrate reductase; NRT, nitrate transporter; PM, plasma membrane; TM, total microsomal; VDAC, voltage-dependent anion-selective channel.

suggesting that they may have specific N uptake and utilization mechanisms. *Salicornia europaea* is one of the most salt-tolerant plant species in the world (Ungar, 1987). A previous study demonstrated that *S. europaea* has a strong ability to utilize N; this plant can thrive under both N-limited and high N conditions (Nie *et al.*, 2012). However, the effect of NaCl on N utilization has not been investigated in *S. europaea*. Elucidating the regulatory networks of efficient N uptake of *S. europaea* under salinity would be helpful for creating salt-tolerant crops with high N use efficiency, which is essential for the development of sustainable agriculture in marginal lands.

N is an essential macronutrient for plant growth. Among various N forms (nitrate, ammonium, amino acids, and peptides), nitrate (NO_3^-) is the predominant form available in aerobic soils (Marschner and Rimmington, 1988). Salinity can severely influence nitrate assimilation in plants. Generally, a high Cl^- concentration acts as an antagonist and represses nitrate uptake; thus, NaCl negatively affects nitrate uptake, assimilation, and protein synthesis which may be responsible, at least in part, for the depressed plant growth under saline conditions (Bar *et al.*, 1997). In addition, the state of the membrane and/or membrane proteins also affects uptake of NO_3^- by altering plasma membrane (PM) integrity under salinity (Frechilla *et al.*, 2001). However, in halophytic *Distichlis spicata* (Pessarakli *et al.*, 2012), NaCl has no negative effect on N uptake. Another report on the euhalophyte *Suaeda physophora* showed that NaCl application significantly increased leaf NO_3^- concentration under N-sufficient conditions (Yuan *et al.*, 2010). In fact, sodium-dependent NO_3^- uptake has been reported in the marine diatom *Phaeodactylum tricornutum* (Rees *et al.* 1980), cyanobacteria (Lara *et al.* 1993), and the marine halophyte *Zostera marina* (Rubio *et al.*, 2005). These results indicated that NaCl may have a promoting effect on nitrate uptake in some halophytes, which is different from glycophytes, whereas the underlying molecular networks are still unclear.

Nitrate uptake occurs in the outer cell layers of roots and relies on nitrate transporters, which are mainly localized at the PM together with the regulatory proteins. To date, four families of nitrate transporters have been identified: nitrate transporter 1/peptide transporter family (NRT1/PTR), nitrate transporter 2 family (NRT2), chloride channel family (CLC), and slow anion channel-associated homologues (SLAC1/SLAH) (Krapp *et al.*, 2014). More than 60 nitrate transporters have been estimated in *Arabidopsis*, the regulation of which involves complex networks that are not fully understood. Investigations on root PM protein accumulation under different NaCl and nitrate levels would significantly enhance our knowledge of nitrate signalling under salinity. Proteomics is a powerful tool to study PM proteins depending on two main approaches, namely gel-free and two-dimensional electrophoresis (2-DE) (Nouri and Komatsu, 2010). The gel-free method has better coverage and higher solubility for hydrophobic membrane proteins than 2-DE. However, proteins containing a single transmembrane domain or peripheral membrane-associated proteins can be more readily resolved in 2-DE. In addition, 2-DE can give information on post-translational modifications (Tang, 2012) and it is also a valuable tool in deciphering N-terminal processing of proteins (Taylor *et al.*, 2011). Nouri and Komastu (2010) used both gel-free and 2-DE methods to study soybean PM proteins, and concluded that the two techniques are complementary for comparative analysis. Meanwhile, Tang *et al.* (2008) used two-dimensional fluorescence difference gel electrophoresis (2D-DIGE) to study *Arabidopsis* PM proteins, and three homologous brasinosteroid-signalling kinases were successfully identified; thus, 2D-DIGE is demonstrated to be a powerful approach for studying signalling proteins localized in the PM.

Proteomic research on glycophytes has focused on PM proteins under salt stress (Cheng *et al.*, 2009). Meanwhile, in a few studies, whole-plant proteomics have been applied in *Arabidopsis* (Wang *et al.*, 2012), *Zea mays* (Prinsi *et al.*, 2009), and barley (Moller *et al.*, 2011) to detect their responses to different N conditions. However, no research has been performed to analyse the PM proteome of halophytes under different nitrate and NaCl levels. The aim of this study was to investigate the characteristics of nitrate uptake in *S. europaea* under NaCl treatment and to identify the underlying regulatory components. Through physiological analysis, it was demonstrated that in contrast to the situation in glycophytes, NaCl facilitates nitrate uptake in *S. europaea*. Comparative proteomics and cell biology studies further revealed that calcium signalling plays important roles in this process. These results open up exciting perspectives for further investigations on the specific regulatory pathways involved in efficient N uptake under NaCl conditions.

Materials and methods

Plant materials and growth conditions

Salicornia europaea seeds were collected from the coastal area of Dafeng City, Jiangsu Province, China. The plants were grown in a greenhouse with a day/night temperature regime of 25 °C/20 °C, photoperiod of 16 h, and relative humidity of ~60%. At 20 d after sowing on perlite granules, seedlings were irrigated with four solutions containing different concentrations of NO_3^- and NaCl in modified 1/2 Hoagland solution for 30 d. Then the plants were harvested and washed with distilled water to remove the surface ions and used for further analysis. The modified 1/2 Hoagland solution contained 0.5 mM KH_2PO_4, 1 mM $MgSO_4$, 2.5 mM $CaCl_2$, 0.05 mM Fe-EDTA, 2.5 mM KCl, and micronutrients, with the pH adjusted to 6.5 ± 0.1. The four treatments were 0.1 mM NO_3^- (LN), 0.1 mM NO_3^- +200 mM NaCl (LN+S), 10 mM NO_3^- (HN), and 10 mM NO_3^- +200 mM NaCl (HN+S).

Measurement of fresh weight (FW), dry weight (DW), root length, and root volume FW was measured immediately after harvesting. DW was measured after drying for 48 h in an oven at 80 °C. Roots were scanned with a digital scanner (Epson, Nagano, Japan) and then analysed with WinRHIZO software (Regent Instruments Inc., Quebec, Canada).

Quantification of total Na, total N contents, and NO_3^- concentrations Plants were dried for 72 h in an oven at 80 °C and then weighted and subsequently ground into powder in a mixer mill (Retsch MM400, Hann, Germany). The powder was digested with a mixture of nitric acid and hydrogen peroxide using a microwave system (MARS; CEM Corporation, Matthews, NC, USA), which was used to determine total Na contents by atomic emission spectrometry (ICP-AES, Thermo, Waltham, MA, USA). N contents were determined by a Vario EL III CHNOS Elemental Analyzer (Elementar Analysensysteme GmbH, Germany). The NO_3^- concentration was measured as previously described (Jampeetong and Brix,

2009). Dried material (5–10 mg) was extracted with 10 ml of Milli Q water at 80 °C in a water bath for 20 min. Then, NO_3^- concentrations were analysed by an AA3 continuous flow-analyser (Seal Analytical, Germany).

Analysis of nitrate reductase (NR) activities NR activities were measured as previously described (Yaneva *et al.*, 2002) with some modifications. The seedlings were homogenized in extraction buffer [50 mM HEPES-KOH, pH 7.5, 1 mM EDTA, 10 mM glutathione (GSH), 0.1% (w/v) polyvinylpyrrolidone (PVP), 1 mM dithiothreitol (DTT), and 1 mM phenylmethylsulphonyl fluoride (PMSF)] and centrifuged for 20 min at 12 000 *g*. The supernatant was incubated with reaction buffer (50 mM HEPES-KOH, pH 7.5, 5 mM KNO_3, 0.2 mM NADH) in the dark at 25 °C for 20 min; the reaction was terminated by addition of 1% sulphanylamide in 1.5 M HCl and 0.01% *N*-(1-naphthyl)-ethylenediammonium dichloride. Nitrite production was determined by reading the absorbance at 540 nm.

Analysis of nitrate uptake rates Nitrate uptake rates were measured as previously described (Muños *et al.*, 2004). *Salicornia europaea* plants of ~30 d old irrigated with 1/2 Hoagland solution plus 200 mM NaCl were transferred to 0.1 mM $CaSO_4$ for 1 min and then to four solutions containing different NaCl and $K^{15}NO_3$ (99% atom excess ^{15}N) concentrations, as follows: 0.1 mM $K^{15}NO_3$, 0.1 mM $K^{15}NO_3$+200 mM NaCl, 10 mM $K^{15}NO_3$, and 10 mM $K^{15}NO_3$+200 mM NaCl for 15 min, and finally, to 0.1 mM $CaSO_4$ for 1 min. Six roots for each treatment and three independent biological replications were dried at 70 °C for 48 h and ground. The powder (2–3 mg) was used for ^{15}N determination by the Delta Plus-MS system (Thermo).

Thirty-day-old *S. europaea* plants irrigated with 1/2 Hoagland solution plus 200 mM NaCl were pre-treated with 1 mM of the non-specific Ca^{2+} channel blocker $LaCl_3$ for 24 h. The $LaCl_3$-pre-treated and control plants were used for $^{15}NO_3^-$ uptake assay following the above-mentioned method.

Plasma membrane (PM) isolation PMs were isolated as previously reported (Tang, 2012). Roots were homogenized in grinding buffer (pH 7.5) (25 mM HEPES, 0.33 M sucrose, 10% glycerol, 0.6% PVP, 5 mM ascorbic acid, 5 mM EDTA, 5 mM DTT, and 1 mM PMSF). The homogenate was filtered through Miracloth and centrifuged at 10 000 *g* for 15 min. Total microsomal (TM) fractions were pelleted by centrifugation at 80 000 *g* for 1 h and resuspended in suspension buffer [5 mM KH_2PO_4/K_2HPO_4 buffer (pH 7.8), 0.33 mM sucrose, 3 mM KCl, 1 mM DTT, and 1 mM protease cocktail]. Two-phase partitioning was performed by using a solution containing 6.2% polyethylene glycol (PEG) 3350, 6.2% dextran T-500, 0.33 M sucrose, 3 mM KCl, and 5 mM KH_2PO_4/K_2HPO_4 buffer (pH 7.8). The mixture was centrifuged at 1500 *g* for 10 min. After partitioning, the upper phase fraction was diluted with 10 vols of dilution buffer (0.33 M sucrose, 25 mM HEPES, and 1 mM DTT) and spun at 120 000 *g* for 1 h to collect the PMs. Then, the PM vesicles were incubated with 0.02% Brij-58 detergent on ice for 10 min to invert the vesicles and release the cytosolic contaminants. Samples were then diluted 20 times with double-distilled H_2O and centrifuged at 120 000 *g* for 60 min (Elmore *et al.*, 2012). The pellets were resuspended in 100 µl of suspension buffer (5 mM KH_2PO_4/K_2HPO_4 buffer, pH 7.8, 3 mM KCl, 1 mM DTT, 0.1 mM EDTA, and 1 µM protease cocktail). For each sample, five independent biological replicates were prepared.

Immunodetection assay and H^+-ATPase hydrolytic activity assay Immunoblot analysis was performed according to standard methods (Zhang *et al.*, 2011). Equal amounts of 5 µg of proteins from TM and PM fractions were separated by SDS–PAGE (Supplementary Fig. S1 availabe at *JXB* online) and transferred to nitrocellulose membranes (GE Amersham Biosciences, NY, USA) using a wet transblot system (Bio-Rad, Hercules, USA). The TM and PM proteins were probed with specific primary antibodies, and visualized using the enhanced chemiluminescence method. The primary antibodies used were anti-H^+-ATPase (PM marker, Agrisera, Vännäs, Sweden), anti-Sar1 [secretion-associated and Ras-related protein 1, an endoplasmic reticulum (ER) marker, Agrisera], and anti-V-ATPase (tonoplast marker, Agrisera).

Hydrolytic activity of the PM H^+-ATPase was measured according to the method of Nouri and Komastu (2010). The PM fraction was added to the reaction solution containing 30 mM MES-TRIS (pH 6.5), 50 mM KCl, 3 mM $MgSO_4$, and 3 mM ATP in the presence or absence of the specific H^+-ATPase inhibitor 0.1 mM Na_3VO_4 and incubated at 30 °C for 15 min. The reaction was stopped by the addition of 0.5% ammonium molybdate, 1% SDS, and 0.4 M H_2SO_4. Ascorbate was then added at a final concentration of 0.3%, the mixture was placed at room temperature for 30 min, and the absorbance was measured at 750 nm.

Labelling of proteins with Cy dye PM proteins were precipitated with the methanol/chloroform method as previously reported (Wessel and Flügge, 1984). The protein pellets were recovered in modified 2D-DIGE buffer (7 M urea, 2 M thiourea, 4% CHAPS, 25 mM TRIS-HCl, and 1% *n*-dodecyl β-D-maltoside). The pH of protein samples was adjusted to 8.8 with HCl and NaOH, and the protein concentration was determined using the Bradford method. The internal standard was prepared by mixing equal amounts of all analysed samples. Protein samples were labelled using minimal fluorescent dyes (Cy3, Cy5, and Cy2) (GE Healthcare, Pittsburgh, PA, USA) following the manufacturer's instruction.

2D-DIGE and image scanning The labelled protein samples were mixed with the internal standard (Supplementary Table S1 at *JXB* online), adjusted to a total volume of 450 µl with rehydration buffer [7 M urea, 2 M thiourea, 4% CHAPS, 1% DTT, and 1% immobilized pH gradient (IPG) buffer, pH 4–7], and used for isoelectric focusing (IEF). IEF was performed on an IPG strip holder with 24 cm, linear gradient IPG strips with pH 4–7 (GE Healthcare) and then on an Ettan DALT System (GE Healthcare) according to the manufacturer's instructions. The images were analysed using DeCyder 6.5 (GE Healthcare). Spots reproducible in 24 of 30 images were used to identify protein abundance change by two-way analysis of variance (ANOVA) ($P<0.05$). The gels used for 2D-DIGE analyses were stained with Coomassie Brilliant Blue (CBB) to observe highly abundant spots. Then, additional gels with 1 mg of internal standard proteins were stained with CBB for spots that could not be determined from 2D-DIGE gels.

Protein identification and database searching The 117 most abundant spots were digested in-gel with bovine trypsin (Roche Molecular Biochemicals, Indianapolis, IN, USA) as described previously (Wang *et al.*, 2007). The ultrafleXtreme matrix-assisted laser desorption ionization-time of flight/time of flight-mass spectrometer (MALDI-TOF/TOF-MS; Bruker Daltonics, Billerica, MA, USA) was used to reveal the MS/MS spectra. The peptides were suspended with 10 µl of 70% acetonitrile (ACN) containing 0.1% trifluoroacetic acid (TFA), and 1 µl was taken and spotted onto the AnchorChip™ MALDI target plate (Bruker Daltonics). Then 1 µl of matrix solution (1 mg ml^{-1} α-cyano-4-hydroxycinnamic acid in 70% ACN containing 0.1% TFA) was spotted after the sample solution dried. All spectra were obtained in positive ion reflection mode under the control of FlexControl 3.3. The matrix suppression was set to deflection, 500 Da. The spectra detection mass range was set at 700–4000 *m/z*. External calibration involved the use of the Bruker standard peptide calibration kit. For each spot, the top 30 strongest intensity peaks in the MS spectra and single-to-noise threshold >6 were automatically selected as precursor ions for MS/MS analysis. MS spectra were acquired with 400 laser shots per spectrum, whereas MS/MS spectra were obtained using 1500 laser shots per fragmentation spectrum. Then MS and MS/MS data were transferred to BioTools 3.2 (Bruker Daltonics) and searched against three databases with the Mascot engine 2.2.03 (http://www.matrixscience.com). The three databases were the NCBInr protein database (http://www.ncbi.nlm.nih.gov/; green plants, 1 669 695 sequences in NCBI 20131226) and two *S. europaea* transcriptome-translated protein databases, as follows: database 1 (162 969 sequences; Ma *et al.*, 2013) and database 2 (35 219 sequences; Fan *et al.*, 2013). Monoisotopic and $[M+H]^+$ were selected for mass values. Peptide mass tolerance was set at 50 ppm, fragment mass tolerance was set as 0.5 Da, and one missing cleavage was permitted. Carbamidomethyl (C) was set as fixed modification and Oxidation (M) was set as variable modification. All proteins were matched by Mascot with scores that exceeded their 95% confidence threshold and contained at least

one peptide with a score at a significance threshold (P<0.05). If several database entries of homologous proteins matched these criteria, only the entry with the highest score is reported. For proteins having only one matching peptide with a score at a significant threshold (P<0.05), the MS/MS spectra were also presented (Supplementary Fig. S3; Supplementary Table S3 at *JXB* online).

Protein classification and bioinformatics analysis The identified proteins were searched against the NCBI protein database (http://www.ncbi.nlm.nih.gov/) and Uniprot (http://www.uniprot.org/) and were divided into different groups based on their molecular and biological functions. The subcellular location of each protein was determined by SUBAIII (http://suba3.plantenergy.uwa.edu.au) and published information on the homologous proteins in *Arabidopsis*. Principal component analysis (PCA) was performed using the extended data analysis module within the DeCyder software (GE Healthcare). Heat map was performed using MultipleExperiment Viewer 4.8.1 software based on the Log_2-transformed fold change.

RNA isolation and quantitative real-time PCR (qRT-PCR) analysis Total RNA was extracted by Trizol reagent and treated with RNase-free DNase I. A 0.5 μg aliquot of RNA was used for the first-strand cDNA synthesis with the SuperScript III first-strand synthesis system (Invitrogen, Carlsbad, CA, USA). qRT-PCR was performed with an Mx3000P Real-Time PCR System (Agilent, USA) using SYBR qPCR Mix (Toyobo, Japan). The relative gene expression levels were calculated by the $2^{-\Delta\Delta CT}$ method, and the α-tubulin gene was used as internal control (Lv *et al.*, 2012). qRT-PCR of each sample was repeated three times. The oligonucleotide primers used are listed in Supplementary Table S5 at *JXB* online.

Detection of $[Ca^{2+}]_{cyt}$ Thirty-day-old *S. europaea* plants irrigated with 1/2 Hoagland solution plus 200 mM NaCl were used. In the 2 h NaCl exposure experiment, the intact roots were incubated in loading solution containing 20 μM Fluo-4/AM, 50 mM sorbitol, 0.2 mM $CaCl_2$, and 0.05% Pluronic F127 (pH 4.2) at 4 °C for 4 h in the dark, followed by a 2 h incubation with 0.2 mM $CaCl_2$ with or without 200 mM NaCl at 20 °C in the dark. In the 24 h, 3 d, and 30 d NaCl exposure experiments, the plants were first pre-treated with 200 mM NaCl for 18 h, 66 h, and 30 d. Then, the intact roots of treated and control plants were incubated in loading solution with or without 200 mM NaCl at 4 °C for 4 h in the dark, after which the roots were incubated for 2 h with 0.2 mM $CaCl_2$ with or without 200 mM NaCl at 20 °C in the dark. After washing with buffer, $[Ca^{2+}]_{cyt}$ was determined under a laser scanning confocal microscope (Leica TCS SP5, Wetzlar, Germany) at excitation and emission wavelengths of 488 nm and 505–530 nm, respectively. Observations were focused on the primary root tips of plants. The same area of root tips of each sample was analysed using Image J software (National Institutes of Health, Bethesda, MD, USA) to determine the fluorescence intensity (mean pixel intensity).

Statistical analysis Statistical analysis was carried out using SPSS 18.0 software. Data were evaluated by two-way ANOVA. To determine the type of interaction between saline and nitrogen treatment, taking the FW for example, the effect of saline–high nitrogen treatment (FW_{HN+S}/FW_{LN}) was compared with the effect of each factor when applied individually (i.e. $FW_{HN}/FW_{LN}\times FW_{LN+S}/FW_{LN}$). Interaction was synergistic if FW_{HN+S}/FW_{LN} was substantially more than $FW_{HN}/FW_{LN}\times FW_{LN+S}/FW_{LN}$; and it was additive if FW_{HN+S}/FW_{LN} was approximately equal to $FW_{HN}/FW_{LN}\times FW_{LN+S}/FW_{LN}$, whereas it was antagonistic if FW_{HN+S}/FW_{LN} was substantially less than $FW_{HN}/FW_{LN}\times FW_{LN+S}/FW_{LN}$ (Striker *et al.*, 2015). For each experiment, at least three replications were used for analysis. The methods of significance testing are described in the figure legends.

Results

NaCl had a synergetic effect with nitrate on the growth of S. europaea

In this study, the effect of NaCl and nitrate on the growth of *S. europaea* was first investigated. Seedlings were treated with four different solutions, LN, LN+S, HN, and HN+S. Generally, NaCl has a positive influence on the growth of euhalophytes, for which zero NaCl is an abnormal condition whereas 200 mM NaCl is in the range of optimal condition (Flowers and Colmer, 2008). Consistently, in this study, it was found that *S. europaea* grows better in the presence of 200 mM NaCl under both LN and HN conditions. In addition, high N also promotes the growth of *S. europaea* (Fig. 1A, B). The FW, DW, root length, and root volume were measured, and two-way ANOVA (P<0.05) was used to reveal the effects of S, N, and S×N on these parameters. All the four traits showed significant S and N effects. The FW and DW increased under NaCl and NO_3^- treatments, and seedlings treated with HN+S exhibited the highest values, whereas LN showed the lowest (Fig. 1C, D). Moreover, a significant S×N interaction was observed for FW and DW, and the type of interaction was synergistic (Fig. 1C, D), suggesting that NaCl and nitrate had synergistic effects on the growth of *S. europaea*. NaCl facilitated the root growth of *S. europaea*, whereas high nitrate inhibited it. Both the root length and volume were largest under LN+S treatment, the values of which were 110.8% and 103.1% higher than those treated with HN, respectively (Fig. 1E, F).

The effects of NaCl on nitrate uptake and assimilation

In order to investigate the effects of NaCl on the nitrate uptake and assimilation, the total Na and total N contents per plant, the N and NO_3^- concentrations in shoot of *S. europaea*, the nitrate uptake rates, and nitrate reductase activities were measured (Fig. 2). All of the traits except NR activities showed significant S, N, and S×N effects. As expected, total Na contents were significantly increased under NaCl treatments, which were also promoted by N treatment (Fig. 2A). Under low N conditions, no significant effect of NaCl on total N content and shoot N concentrations was observed (Fig. 2B, C), but the shoot NO_3^- concentrations and the nitrate uptake rates increased significantly by NaCl treatment. The values increased by 83.4% and 32.8% (Fig. 2D, E), respectively. Compared with the LN condition, NR activity under LN+S increased by 23.5%, but the values were very low and the difference was not statistically significant (Fig. 2F). Under high N conditions, the shoot N concentrations were significantly decreased by NaCl treatment (Fig. 2C), but the total N contents, shoot NO_3^- concentration, the nitrate uptake rates, and the NR activities were all significantly increased by NaCl treatment. The values increased by 27.8, 14.6, 57.6, and 41.7%, respectively (Fig. 2B–F). Notably, NaCl and NO_3^- also had a synergistic interaction effect on nitrate uptake rate. These results showed that NaCl could promote nitrate uptake and assimilation in *S. europaea*.

Identification of NaCl- and nitrate-regulated PM proteins by 2D-DIGE

To determine the proteins regulated by NaCl and nitrate in *S. europaea*, a comparative proteomic analysis of root PM proteins under the four treatments was conducted. Root PM

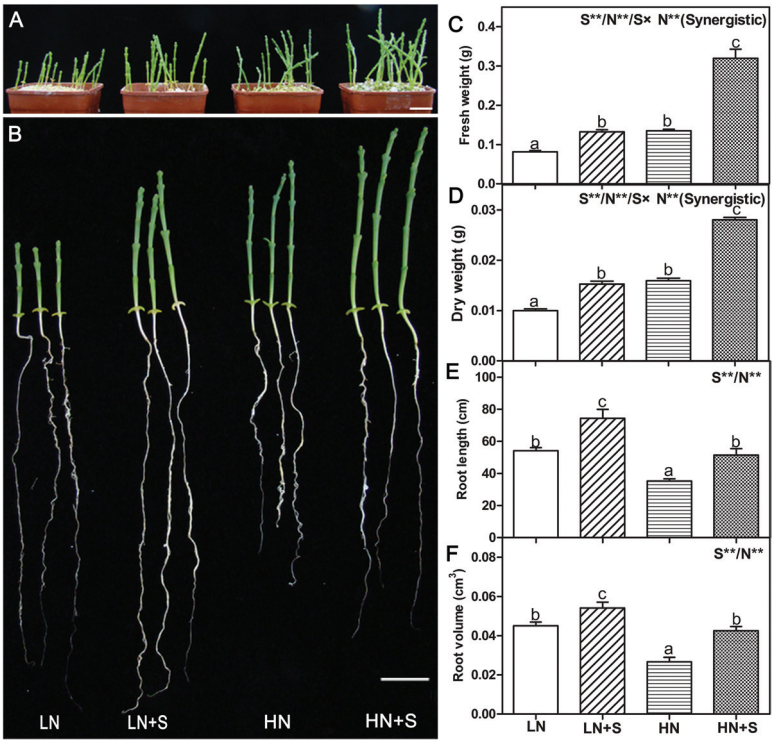

Fig. 1. Phenotypic and physiological changes of *S. europaea* grown under different NaCl and NO_3^- concentrations. *S. europaea* seedlings were treated with different nitrate and NaCl concentrations for 30 d, and the phenotypes (A and B), fresh weight (C), dry weight (D), root length (E), and root volume (F) were determined. Scale bars=2 cm. Values were means ±SE (n=12). Different letters above the bars indicated significant differences (P<0.05). For C, D, E, and F, two-way ANOVA was performed to indicate significant S, N, and S×N effects. Double asterisks indicate significant differences at P<0.01. Combined effects are symbolized by a slash (/). Synergistic indicates the type of interaction.

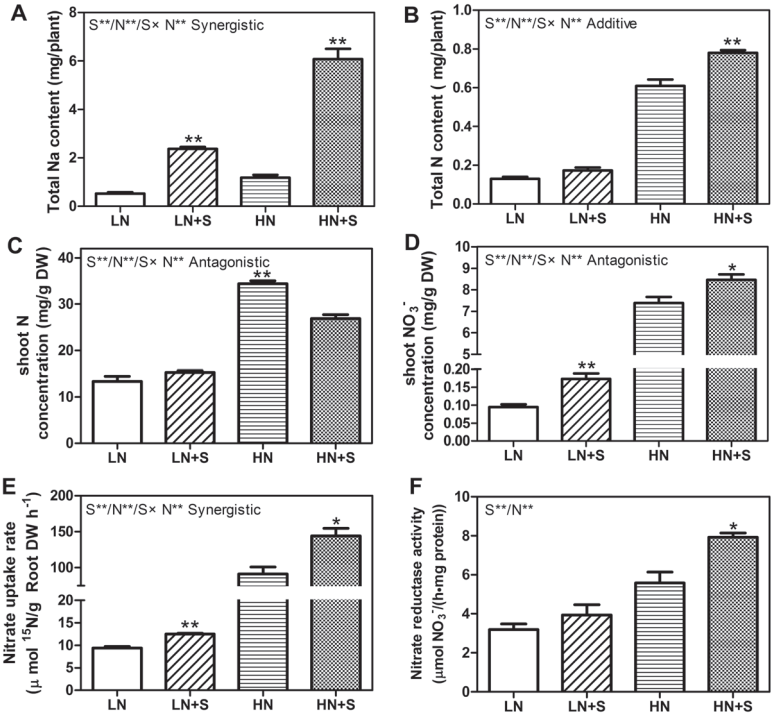

Fig. 2. Total Na and N contents, shoot N and NO_3^- concentrations, nitrate uptake rates, and NR activities of *S. europaea* grown under different NaCl and NO_3^- concentrations. *S. europaea* seedlings were treated with different nitrate and NaCl concentrations for 30 d, total Na (A) and total N (B) content of the whole plant, shoot N (C) and NO_3^- (D) concentration, and NR activity (F) were measured. (E) *S. europaea* seedlings were treated with four different NaCl and ^{15}N labelled $K^{15}NO_3$ concentrations for 15 min, and the content of ^{15}N in roots was measured. Values were means ±SE (n=4 for A, B, C, D, and F; and n=3 for E). Asterisks indicate significant differences (P<0.05) between salt-treated and untreated samples. In addition, two-way ANOVA was performed to indicate significant S, N, and S×N effects. Double asterisks indicate significant differences at P<0.01, and combined effects are symbolized by a slash (/). Synergistic, additive, and antagonistic represent different types of interaction.

fractions were purified by the two-phase partitioning method (Tang, 2012), and their purity was evaluated by western blot analysis. Compared with the TM fraction, H^+-ATPase was strongly enriched in the PM fraction. Conversely, V-ATPase, a tonoplast membrane protein, was more strongly enriched in the TM fraction than in the PM fraction. Sar1, an integral ER membrane protein, was only detected in the TM fraction and was absent in the PM fraction (Fig. 3A). Furthermore, the hydrolytic activity of PM H^+-ATPase in the presence or absence of 0.1 mM of the specific PM H^+-ATPase inhibitor Na_3VO_4 was determined, and the purity of PM vesicles was 84.76 ± 2.80%. These results demonstrated that PM vesicles of relatively high purity were obtained.

2D-DIGE with pH 4–7 strips was used to separate root PM proteins, and ~2400 protein spots were found in each image (Fig. 3B; Supplementary Fig. S2 at *JXB* online). The 20 protein samples representing five biological repeats of each of the four treatments were assigned to 10 DIGE gels, which were labelled with Cy2, Cy3, and Cy5. A total of 30 images were acquired (Supplementary Table S1; Supplementary Fig. S2). After matching the 30 spot maps, 717 protein spots were found in 80% of them (Supplementary Table S2). PCA based on these 717 protein spots was performed to determine the distribution and similarities of different experimental groups. The five spot maps of each treatment were exactly clustered in the score plot (Fig. 4A), indicating high reproducibility among the replicate gels. Principal component 1 (PC1) explained 47.7% of the variance and separated the experimental groups according to NaCl treatment, whereas the axis PC2 accounted for 13.7% of the variance and separated the experimental groups according to nitrate treatment.

Two-way ANOVA (P<0.05) with false discovery rate (FDR) correction for multiple testing revealed that a total of 406 spots displayed significant S, N, and S×N effects and at least one absolute variation >1.5-fold by comparison within the different treatments. Overall, among the differentially accumulated proteins, 166, 18, and 14 spots displayed pure S, N, and S×N effects, respectively, showing that NaCl treatment had a greater impact on protein accumulation than nitrate. In addition, 69 spots displayed pure combined S and N effects, which indicated that both NaCl and nitrate affected

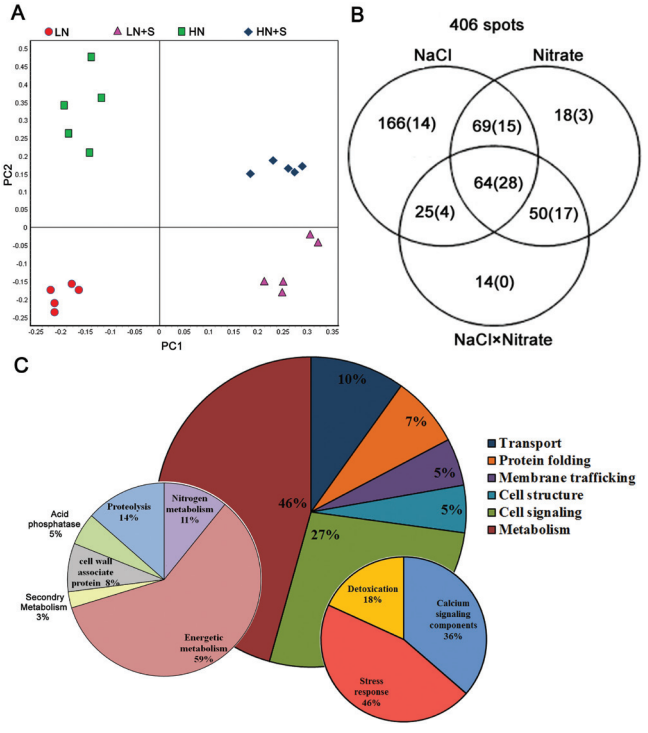

Fig. 4. PCA, spot significant analysis, and functional classification of the identified proteins. (A) PCA of the different experimental groups. Samples plotted on the first two principal components (PCs) are shown. (B) Venn diagram showing the distribution of significant spots following two-way ANOVA. The numbers outside the parentheses are the total numbers of significant spots and at least one absolute variation was obtained above 1.5-fold by performing comparisons among the different treatments. The numbers in parentheses are the number of protein spots identified in the MALDI-TOF/TOF-MS. (C) Functional classification of 81 identified proteins. The percentage of proteins from each category is shown. The two most abundant categories, metabolism and cell signalling, were subsequently divided into subgroups.

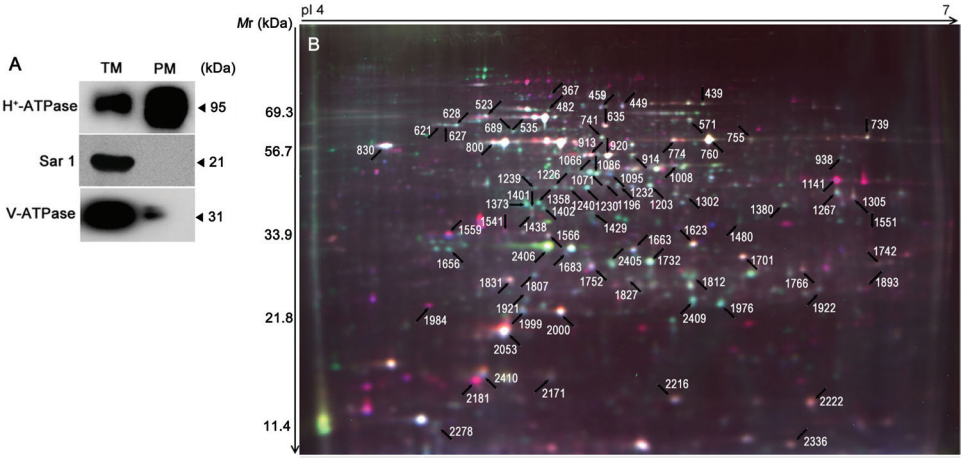

Fig. 3. Purity assessment and a representative 2D-DIGE image. (A) Western blot analysis of extracted PM proteins with antibodies against proteins from different cell compartments. (B) PM proteins were separated by 2D-DIGE and detected with a Typhoon 9400 Scanner. The differentially accumulated protein spots under different NaCl and nitrate concentrations were determined using two-way ANOVA, and those positively identified by MALDI-TOF-TOF are marked by arrows.

the accumulation of these proteins, but the two factors were independent. Finally, 64 spots displayed significant S×N effect in combination with S and N effects, indicating that NaCl and nitrate had interactive effects on the accumulation of these proteins (Fig. 4B).

Functional classification of NaCl- and nitrate-regulated proteins

After removing the dim spots and noise, the 117 most abundant spots displaying significant S, N, and/or S×N effects were manually excised from the gels, and further analysed by MS/MS spectra. Since there is a lack of information on the genome and comprehensive protein sequence *of S. europaea*, these spectra were searched against the NCBInr green plant database and two *S. europaea* transcriptome-translated protein databases (Fan *et al.*, 2013; Ma *et al.*, 2013). Most proteins blasted by the three databases were homologous proteins from different species, and the ones with the highest scores were finally selected for annotation (Supplementary Fig. S3; Supplementary Table S3 at *JXB* online). In total, 81 out of the 117 spots were annotated, among which 65 proteins have been previously shown or predicted to be associated with the PM. The localization information determined by the SUBAIII database and the literature is listed in Supplementary Table S3.

Furthermore, the identified proteins were grouped into six categories based on their molecular and biological functions, namely metabolism (46%), cell signalling (27%), transport (10%), protein folding (7%), membrane trafficking (5%), and cell structure (5%). The two major categories were further classified into subcategories. Specifically, proteins related to metabolism were divided into six subcategories, as follows: N metabolism, energetic metabolism, secondary metabolism, acid phosphates, cell wall-associated proteins, and proteolysis. Proteins involved in cell signalling were assigned to three subcategories, as follows: calcium signalling components, stress response, and detoxication (Fig. 4C; Supplementary Table S3 at *JXB* online).

The accumulation pattern of the identified proteins

The 81 annotated, differentially accumulated proteins were further grouped into eight distinct clusters (Clusters I–VIII, Fig. 5; Supplementary Table S4 at *JXB* online) according to their change in abundance pattern. These clusters were illustrated by reaction norm diagrams consisting of a graphical representation highlighting the contribution of NaCl treatment (0 mM and 200 mM) to the observed protein abundance for different levels of nitrate treatments (0.1 mM and 10 mM). Cluster I contained 16 proteins whose accumulation increased significantly by NaCl treatment under both LN and HN conditions. Seven of these proteins were also significantly changed under nitrate treatments. Cluster II comprised nine proteins that were significantly repressed by the NaCl treatment under both LN and HN conditions. Four of these nine proteins changed significantly under nitrate treatments. Clusters III and IV comprised proteins whose abundance was increased or decreased significantly by NaCl treatment, but only under HN conditions. Cluster III included 10 proteins, three of which were significantly changed under nitrate treatments. Cluster IV contained six proteins, all of which were significantly changed under nitrate treatments. The largest cluster (Cluster V) comprised 19 proteins, which showed increased accumulation by NaCl treatment under LN conditions. Sixteen of these 19 proteins were also significantly changed under nitrate treatments. Only one protein in Cluster VI was repressed by NaCl treatment under LN conditions, and this protein was also down-regulated under nitrate supplement without NaCl. Cluster VII comprised seven proteins showing opposite responses to NaCl under LN and HN conditions. All of these proteins displayed a clear S×N interaction effect. Cluster VIII comprised 13 proteins whose abundance was not changed significantly by NaCl treatment whether under LN or HN conditions, but the abundance of such proteins changed significantly in response to nitrate.

The involvement of Ca^{2+} signalling in NaCl-facilitated nitrate uptake in S. europaea

Eight calcium signalling components were identified by 2D-DIGE, and seven of these components were up-regulated, whereas the other one was down-regulated by NaCl treatment under HN and/or LN conditions (Fig. 6). qRT-PCR was performed to examine whether the eight components were also regulated at the transcription level. As shown in Fig. 6, the mRNA transcripts of the eight proteins were all up-regulated by NaCl treatment under HN and/or LN conditions. Two of them, annexin (ANN)-like protein RJ4-like and PBI41 14-3-3, displayed consistency between mRNA and protein variation trends, whereas the other six proteins showed some discrepancies (Fig. 6).

Previous studies have shown that $[Ca^{2+}]_{cyt}$ fluctuations and the downstream calcium signalling proteins play pivotal roles in stress responses (Plieth, 2005). Thus, the dynamic changes of $[Ca^{2+}]_{cyt}$ under 200 mM NaCl treatment were determined in *S. europaea* roots using the Ca^{2+}-sensitive fluorescent probe, Fluo-4/AM. In contrast to weak fluorescence detected in the control root tips, strong fluorescence was observed in roots treated with NaCl for 2 h, 24 h, and 3 d (Fig. 7A, B). Although the fluorescence from 30 d NaCl-treated root tips was weak, it was still significantly higher than that of the control. Statistical analysis of the mean intensity of fluorescence showed that $[Ca^{2+}]_{cyt}$ was significantly elevated under NaCl treatments (Fig. 7B).

To investigate the effects of $[Ca^{2+}]_{cyt}$ on nitrate uptake under NaCl treatments in *S. europaea*, $LaCl_3$ (a Ca^{2+} channel blocker) was applied to *S. europaea* roots, and the nitrate influx rates were detected. Pre-treatment with $LaCl_3$ resulted in decreased $[Ca^{2+}]_{cyt}$ (Supplementary Fig. S4 at *JXB* online), and the nitrate uptake rates of roots were significantly reduced under the three treatments besides the HN conditions compared with the control. Moreover, the reduction was much more pronounced under NaCl treatments than without NaCl treatments. After $LaCl_3$ pre-treatment, no significant difference in the nitrate uptake rate was observed between LN and LN+S, or between HN and HN+S (Fig. 7C). This result indicated that the decrease in $[Ca^{2+}]_{cyt}$ not only caused a decrease in nitrate uptake rate, but also attenuated the promotion effects of NaCl on this parameter.

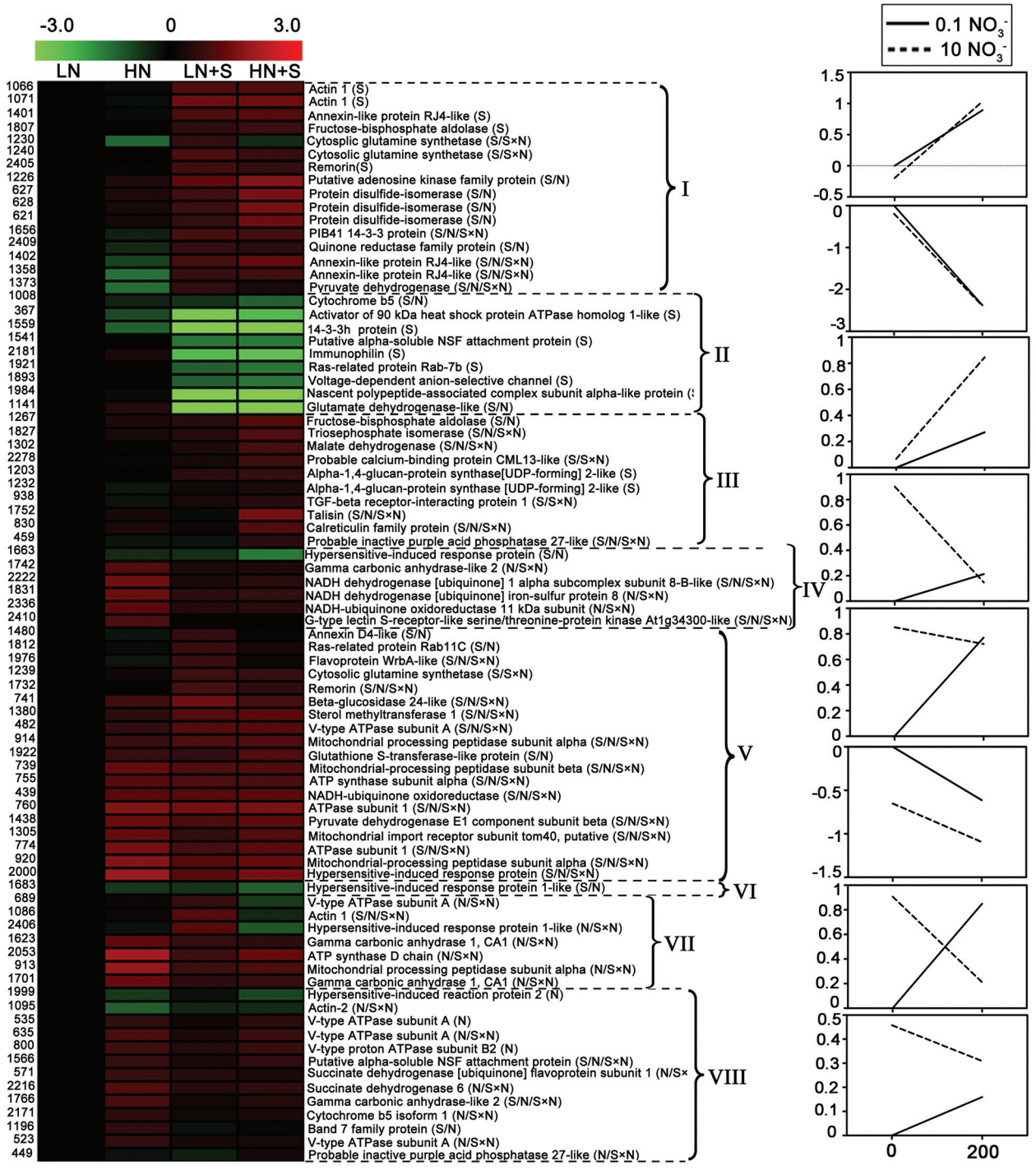

Fig. 5. Clustering analysis of differentially accumulated proteins. The 81 differentially accumulated proteins were grouped into eight clusters according to their change patterns, which are illustrated by reaction norm diagrams consisting of a graphical representation highlighting the contribution of NaCl treatment to the observed protein abundance under nitrate treatment. Each row in the heat map indicates a single protein, whose expression values were generated using Log_2 ($\overline{RV}_{treatments}/\overline{RV}_{LN}$). For each protein, the spot number and the protein name with its ANOVA effect (S, N, and/or S×N) are shown. Reaction norms were generated using the means of Log_2 ($\overline{RV}_{treatments}/\overline{RV}_{LN}$) of spots for each defined cluster. $\overline{RV}$, means of normal volume/normal standard volume.

Discussion

NaCl facilitates nitrate uptake in S. europaea

Generally, NaCl has inhibitory effects on nitrate assimilation in glycophytes. For example, in *Arabidopsis*, NO_3^- concentrations and NR activity in both leaves and roots were markedly decreased by NaCl during the second week of treatment (Debouba *et al.*, 2013). However, in this study, it was found that NaCl can promote nitrate uptake in the euhalophyte *S. europaea*. The shoot NO_3^- concentration and nitrate uptake rates of *S. europaea* were significantly promoted by NaCl under both low N and high N conditions (Fig. 2D, E).

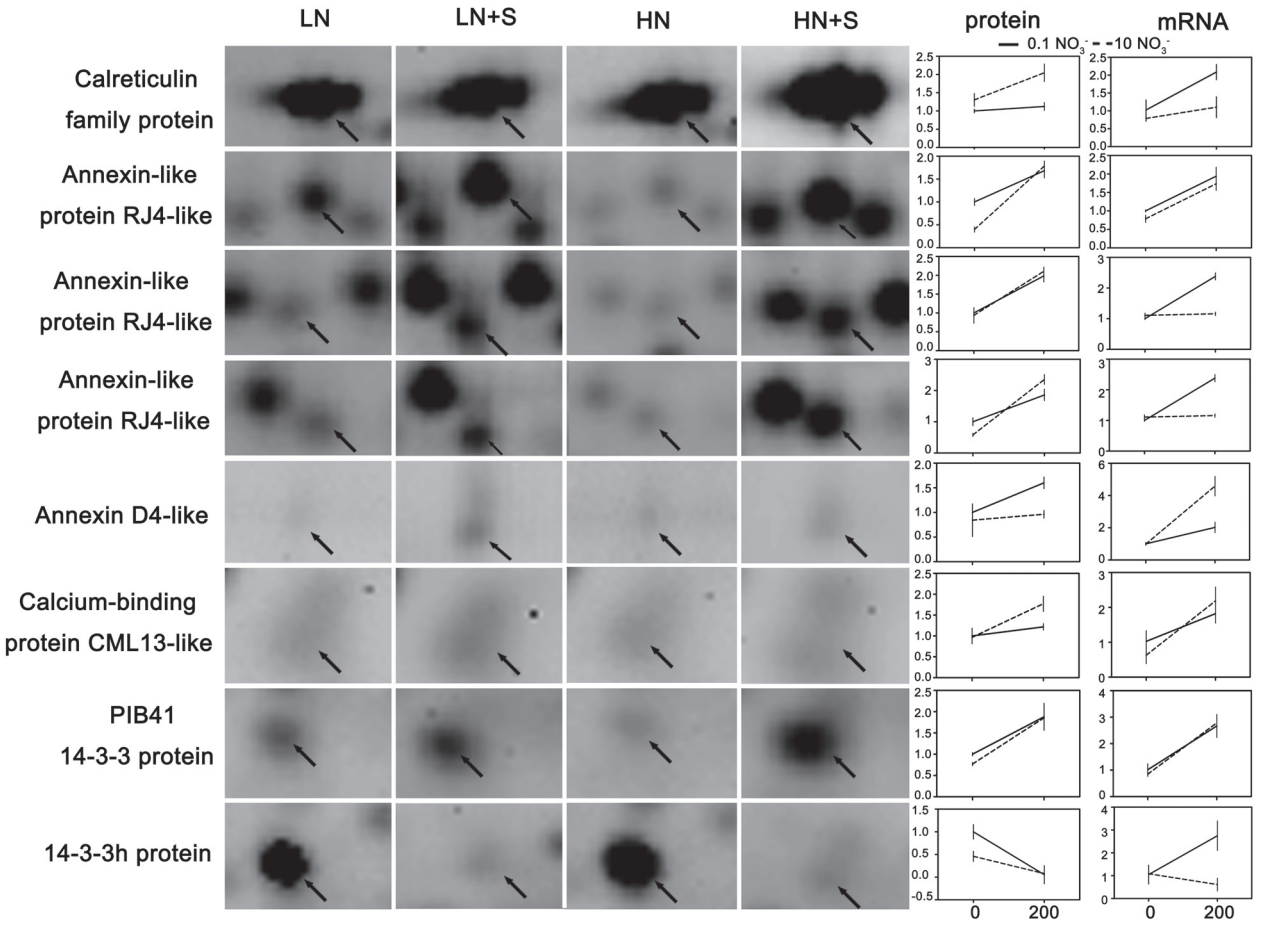

Fig. 6. Expression profiles of calcium signalling components at protein and mRNA levels in response to NaCl and nitrate. The images on the left are magnified views of 2D-DIGE gel sections containing the spot of the calcium signalling components. The corresponding expression files at protein and mRNA levels are listed on the right. Expression levels of mRNAs were evaluated using qRT-PCR, *n*=3. The protein expression values were generated using ($\overline{RV}_{treatments}/\overline{RV}_{LN}$). $\overline{RV}$, means of normal volume/normal standard volume, *n*=5. Values are means ±SD.

These results are consistent with the findings for the euhalophyte *S. physophora* which showed that NaCl application significantly increased the leaf NO_3^- concentration under N-sufficient conditions (Yuan *et al.*, 2010). The current results and previous studies together show that the effect of NaCl on nitrate uptake and assimilation may be significantly different between glycophytes and halophytes. NaCl generally has a positive influence on the growth of euhalophytes, for which zero NaCl is an abnormal condition whereas 200 mM NaCl is in the range of the optimal condition (Flowers and Colmer, 2008). Previous studies showed that the growth of *S. europaea* is stimulated by 200–400 mM NaCl (Wang *et al.*, 2009; Lv *et al.*, 2012). Consistently, in this study, it was found that supply of 200 mM NaCl improved the growth of *S. europaea* under both LN and HN conditions (Fig. 1A, B). Better growth of *S. europaea* under salt conditions increased the demand for N, which could at least partly explain the stimulation of nitrate uptake and increased plant N content by salt treatment (Fig. 2B, E). Furthermore, there might be an NaCl-facilitated nitrate uptake mechanism in *S. europaea*, which is directly supported by the findings that nitrate uptake rates and shoot NO_3^- concentrations of *S. europaea* were significantly promoted by NaCl treatment under both high N and low N conditions (Fig. 2D, E). In addition, the NR activities were significantly increased by salt under the high N condition (Fig. 2F). Consistent with this study, a sodium-dependent nitrate transport at the PM of leaf and root cells was also reported in *Zostera marina*, which is a seagrass that grows submerged in seawater where the NaCl concentration is ~500 mM (Rubio *et al.*, 2005).

The possible roles of Ca^{2+} signalling proteins identified by comparative proteomics in S. europaea

Ca^{2+} plays vital roles in plant development and in response to environmental stimuli (DeFalco *et al.*, 2010). Developmental and environmental cues are perceived at the cell surface, thereby eliciting $[Ca^{2+}]_{cyt}$ changes through concerted action of channels, pumps, and carriers (Kudla *et al.*, 2010). Two protein families, ANN and calreticulin (CRT), involved in this process were identified in this proteomic study. ANN encodes unconventional calcium-permeable channels, which is a key component of root cell adaptation to salinity (Davies, 2014). Four ANN proteins (spots 1358, 1401, 1402, and 1480) were significantly increased in response to NaCl (Fig. 6), indicating that they may act as NaCl-regulated Ca^{2+}-permeable channels in *S. europaea*. Interestingly, spots 1401 and 1402 represented the same protein, which have the same molecular mass

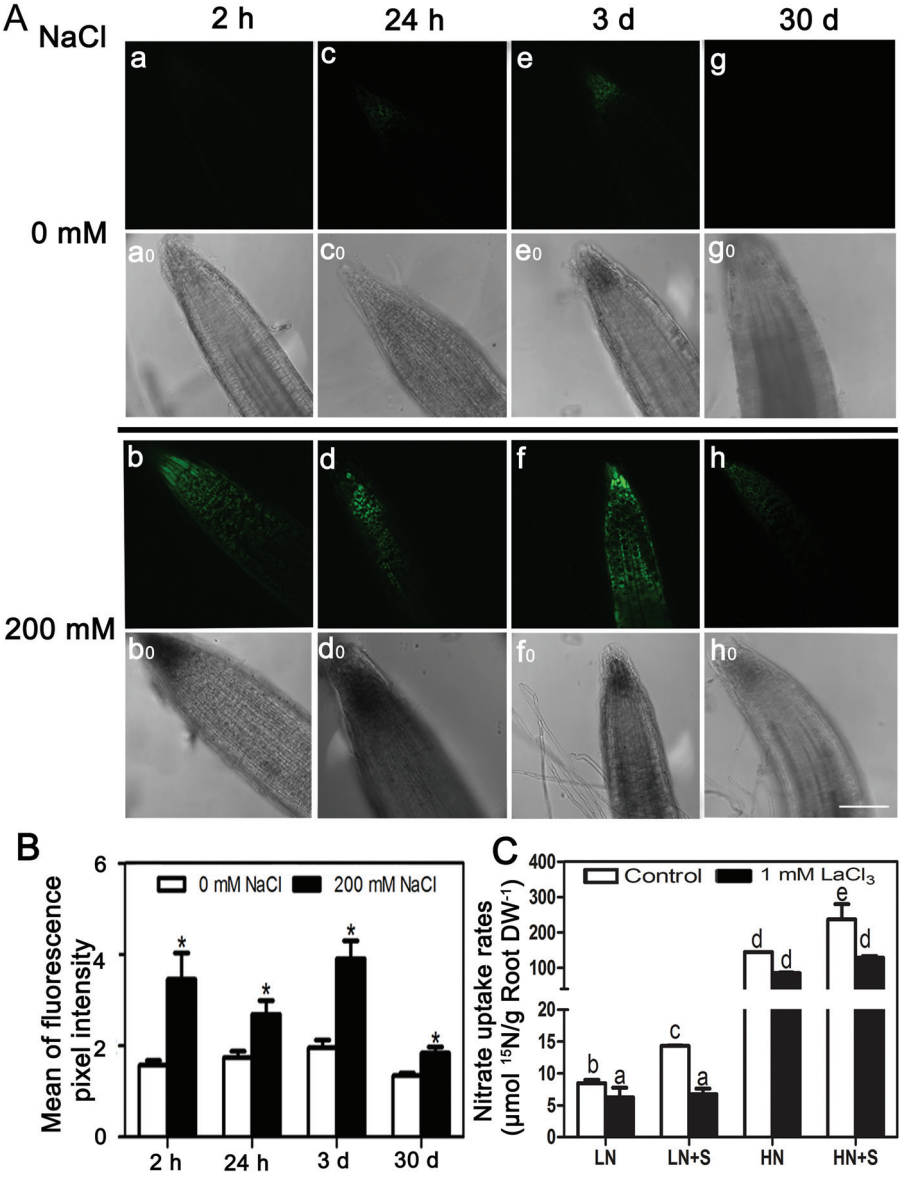

Fig. 7. The involvement of Ca^{2+} signalling in NaCl-facilitated nitrate uptake in *S. europaea*. (A) The effects of NaCl on relative $[Ca^{2+}]_{cyt}$ in *S. europaea* root tips. *S. europaea* seedlings treated with 200 mM NaCl for 2 h, 24 h, 3 d, and 30 d were incubated with Fluo-4/AM, and root tips were observed by confocal microscopy (b, d, f, and h). The root tips without NaCl treatments served as controls (a, c, e, and g), a0 to h0 are light field images of the corresponding root tip. Scale bar=100 μm. (B) Quantification of average fluorescence intensities of root tips. Values are means ±SE (n=10). Asterisks indicate significant differences (P<0.05). (C) The effect of $LaCl_3$ on nitrate uptake rates of *S. europaea* roots. $LaCl_3$-pre-treated *S. europaea* seedlings were immersed in modified 1/2 Hoagland solutions with different NaCl and ^{15}N-labelled KNO_3 concentrations for 15 min, and the content of ^{15}N in roots was measured. Values are means ±SE (n=3). Different letters above the bars indicate significant differences at P<0.05, which were calculated separately under LN and HN conditions.

but different pI values (Fig. 3B). It is speculated that the isoforms may be generated by phosphorylation of ANN. CRT is a highly conserved Ca^{2+}-binding protein functioning in intracellular Ca^{2+} homeostasis and signalling and is predominantly located in the ER; CRT is reportedly associated with the extracellular membrane surface (Jia *et al.*, 2009). CRT is an NaCl-responsive protein in potato (Aghaei *et al.*, 2008), as well as in *Arabidopsis* (Jiang *et al.*, 2007). In *S. europaea*, the abundance of CRT (spot 830) was up-regulated by NaCl only under HN conditions, and it was also induced by HN under NaCl application (Fig. 6), indicating that CRT may act as an NaCl- and HN-responsive protein in *S. europaea* regulating calcium homeostasis and signalling transduction.

The spatio-temporal Ca^{2+} signals are then decoded and transmitted by Ca^{2+}-binding proteins (DeFalco *et al.*, 2010). Calmodulin (CaM)-like (CML) and 14-3-3 proteins involved in this process were identified. CMLs are involved in Ca^{2+} signal transduction by associating with numerous downstream targets, such as protein kinase, phosphatases, transcription factors, transporters, and channels (Popescu *et al.*, 2007). CMLs have been implicated in plant development processes and abiotic stress responses (Magnan *et al.*, 2008). In this study, one CML13-like protein was up-regulated by NaCl under HN conditions (Fig. 6), and this protein may function in Ca^{2+} signalling as a part of the response of *S. europaea* to NaCl under N-sufficient conditions. In

contrast, the accumulation of CML was significantly down-regulated after 48 h salt treatment in roots of barely, which was accompanied by significant reduction of root Ca^{2+} content (Wu *et al.*, 2014). These different trends may reflect diverse mechanisms of CML regulation in glycophytes and halophytes. 14-3-3 proteins are also involved in Ca^{2+} signalling, which can interact with Ser/Thr-phosphorylated proteins (Pauly *et al.*, 2007). They have been reported to regulate plant N assimilation by tuning the activities of NRT2, NR, and glutamine synthase (GS). Two phosphorylation sites of NRT2.1 were identified as being regulated by NaCl treatment (Vialaret *et al.*, 2014), and sequence analysis of NRT2s in tobacco and *Arabidopsis* has identified some possible 14-3-3-binding sites (Guo *et al.*, 2011). The activities of cytosolic NR and GS, the key enzymes in nitrate assimilation, are regulated through phosphorylation by 14-3-3s, calcium-independent protein kinases (CIPKs), and calcium-dependent protein kinases (CDPKs) (Masclaux-Daubresse *et al.*, 2010). NR is the target of CPK17 and 14-3-3, which is regulated by salt stress (Lambeck *et al.*, 2010). Notably, the two 14-3-3 proteins identified in this study changed oppositely in response to NaCl treatment (Fig. 6). Similarly, in salt-tolerant rice strains, the abundance of two 14-3-3 proteins increased, whereas one 14-3-3 protein decreased under salt stress (Liu *et al.*, 2014). These findings indicate that NaCl may regulate 14-3-3 proteins through multiple mechanisms.

Changes in $[Ca^{2+}]_{cyt}$ and downstream Ca^{2+} signalling are essential for NaCl-facilitated nitrate uptake in S. europaea

Salt stress is first perceived at the cell membrane level, and then an intracellular signalling cascade is triggered via secondary messengers (Kader and Lindberg, 2010). The present results suggested that Ca^{2+} acted as an essential second messenger in NaCl-facilitated nitrate uptake in *S. europaea* and functioned through downstream signalling components. First, $[Ca^{2+}]_{cyt}$ was significantly elevated in *S. europaea* under both short- and long-term NaCl treatment (Fig. 7A, B). Many studies have revealed an increase in $[Ca^{2+}]_{cyt}$ after salt stress (Kader *et al.*, 2007; D'Onofrio and Lindberg, 2009). NaCl induces a higher increase in $[Ca^{2+}]_{cyt}$ in salt-tolerant rice cultivars than in salt-sensitive cultivars (Kader *et al.*, 2007). However, in *Arabidopsis* root cells or corn root protoplast, NaCl induced a decrease in $[Ca^{2+}]_{cyt}$ within minutes (Lynch and Läuchli, 1988; Halperin *et al.*, 2003). Thus, the regulation of $[Ca^{2+}]_{cyt}$ by NaCl varies with the tested species, cells, and tissues. It is likely that the amplitude, frequency, and duration of changes in $[Ca^{2+}]_{cyt}$ are important for decoding the specific downstream responses for salt stress response in plants. Secondly, a decline in $[Ca^{2+}]_{cyt}$ not only caused a decrease in nitrate uptake rate, but also eliminated the promotion effects of NaCl on this parameter (Fig. 7C), suggesting that the NaCl-induced $[Ca^{2+}]_{cyt}$ elevation was essential for NaCl-facilitated nitrate uptake in *S. europaea*. Evidence on the direct relationship between $[Ca^{2+}]_{cyt}$ and nitrate uptake is still lacking, but some research has shown links between them. Application of Ca^{2+} could increase nitrate uptake under salt stress, and this effect may be ascribed to its involvement in preserving the structural and functional integrity of cell membranes or in increasing the activities of nitrate transporters (Mansour, 2000). Meanwhile, plants treated with EGTA (a specific Ca^{2+} chelator) or La^{3+} (a Ca^{2+} channel blocker) showed decreased induction of the key genes involved in the nitrate assimilatory pathway, such as NR and nitrite reductase (NiR) (Vidal *et al.*, 2010). Thirdly, eight calcium signalling proteins were identified in this proteomic study, seven of which were significantly up-regulated under NaCl treatments (Fig. 6); it is speculated that these may play important roles in NaCl-facilitated nitrate uptake in *S. europaea*. The important roles of Ca^{2+} signalling proteins in salt adaption have been reported in other plant species. In *Arabidopsis*, the phosphorylation levels of CPKs changed significantly under salt stress (Vialaret *et al.*, 2014). Mehlmer *et al.* (2010) also reported that CPK3-mediated Ca^{2+} signalling is required for salt stress acclimation, and 28 potential CPK3 targets were identified by their studies. Among these, remorin, CRT, VDAC (voltage-dependent anion channel), 14-3-3 proteins, and RAB GTPase, all of which play roles in cellular ion homeostasis and signal transduction under salt stress (Mehlmer *et al.*, 2010), were also identified in the present study. In addition, Latz *et al.* (2013) reported that the vacuolar two-pore K^+ channel 1 (TPK1) was a target of CPK3 and 14-3-3 protein, and played an essential role in the regulation of the cytosolic K^+/Na^+ ratio under salt stress adaptations.

Based on the present results and previous studies, a possible regulatory network of NaCl-facilitated nitrate uptake in *S. europaea* focusing on the involvement of Ca^{2+} signalling is proposed (Fig. 8). In *S. europaea* roots, the NaCl stimuli induced Ca^{2+} entry across the PM by activating ANN protein and some unknown Ca^{2+} channels (Davies, 2014), thereby causing $[Ca^{2+}]_{cyt}$ elevation. CRT is involved in cytosolic Ca^{2+} homeostasis (Jia *et al.*, 2009). The $[Ca^{2+}]_{cyt}$ elevation is sensed by calcium signalling proteins including CaM/CML, CBL/CIPKs, as well as CDPKs/CPKs (DeFalco *et al.*, 2010). 14-3-3 protein can be activated by CPK3 or some unknown Ca^{2+} signalling components (Mehlmer *et al.*, 2010). The calcium signalling proteins can transmit the signal into phosphorylation cascades capable of modulating gene expression, and target protein activity, which may function in ion transport/homeostasis, membrane trafficking, redox homeostasis, and so on (DeFalco *et al.*, 2010). Thus, the elevated nitrate uptake rates and NR activity under NaCl treatment in *S. europaea* may be ascribed to calcium-dependent phosphorylation of proteins such as those described in the following sentences. CBL1/9 and CIPK8/23 are involved in the regulation of NRT1.1 by phosphorylation (Ho *et al.*, 2009; Hu *et al.*, 2009), while 14-3-3 is involved in the regulation of NRT2s (Guo *et al.*, 2011). NRs in the cytosol are targets of CPK17 and 14-3-3, which are also regulated by salt stress (Lambeck *et al.*, 2010). The subsequent steps of N assimilation in roots take place in plastids. GS participates in this processs and can be regulated by CIPK and 14-3-3 through phosphorylation (Masclaux-Daubresse *et al.*, 2010).

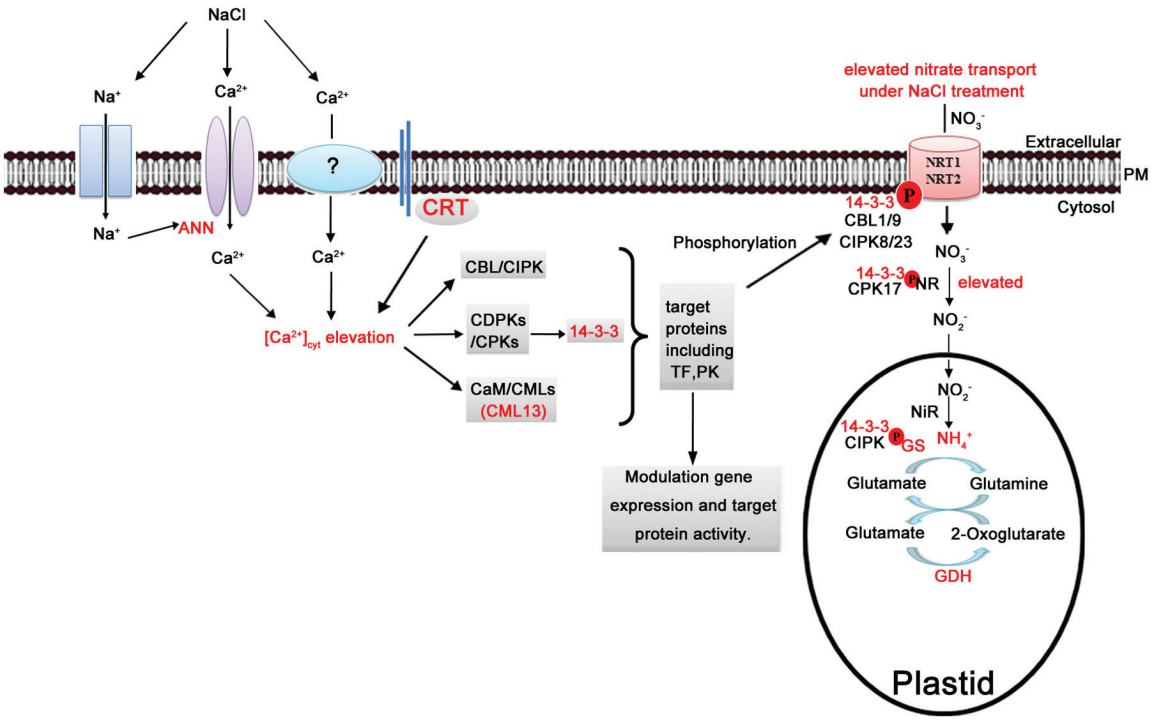

Fig. 8. A putative regulatory network of NaCl-facilitated nitrate uptake in *S. europaea*. In *S. europaea* roots, the NaCl stimuli induced Ca^{2+} entry across the PM by activating ANN protein and some unknown Ca^{2+} channels, thereby causing $[Ca^{2+}]_{cyt}$ elevation. CRT is involved in cytosolic Ca^{2+} homeostasis. The $[Ca^{2+}]_{cyt}$ elevation is sensed by calcium signalling proteins including CaM/CML, CBL/CIPKs, and CDPKs/CPKs. 14-3-3 protein can be activated by CPK3 or some unknown Ca^{2+} signalling components. The calcium signalling proteins can transmit the signal into phosphorylation cascades capable of modulating gene expression and target protein activity, which may function in ion transport/homeostasis, membrane trafficking, redox homeostasis, and so on. CBL1/9 and CIPK8/23 are involved in the regulation of NRT1.1 by phosphorylation while 14-3-3 is involved in the regulation of NRT2s. NRs in the cytosol are targets of CPK17 and 14-3-3, which are also regulated by salt stress. The subsequent steps of N assimilation take place in plastids. GS participates in this process and can be regulated by CIPK and 14-3-3 through phosphorylation. The components in red indicate those identified in the present study.

Conclusions

In this study, it was first found that, unlike in glycophytes, NaCl facilitates nitrate uptake in *S. europaea*, which may be a unique feature in halophytes. Further comparative proteomics of root PM proteins revealed 81 differentially accumulated proteins in response to salt and nitrate. Among them, there are eight calcium signalling components, and the accumulations of seven was increased in response to salinity. $[Ca^{2+}]_{cyt}$ was significantly elevated in *S. europaea* under both short- and long-term NaCl treatment. In addition, application of the Ca^{2+} channel blocker $LaCl_3$ not only caused a decrease in nitrate uptake rate but also reduced the promotion effects of NaCl on the nitrate uptake rates. It is proposed that NaCl induced $[Ca^{2+}]_{cyt}$ elevation and the downstream calcium signalling are essential for NaCl-facilitated nitrate uptake in *S. europaea*. The calcium signalling proteins may function through regulating the expression or activity of nitrate transporters and some key enzymes in N assimilation, which can consequently affect nitrate assimilation.

Supplementary data

Supplementary data are available at *JXB* online.

Figure S1. Coomassie blue-stained gel image of TM and PM samples.

Figure S2. Ten images of 2D-DIGE.

Figure S3. Scores and matched peptides of the identified proteins based on ultrafleXtreme MALDI-TOF/TOF-MS.

Figure S4. The effect of $LaCl_3$ on the relative $[Ca^{2+}]_{cyt}$ in *S. europaea* root tips.

Table S1. Protein samples assigned for Cy dye label and DIGE.

Table S2. Expression profile data of the 717 spots present in at least 24 of the 30 images.

Table S3. The differentially accumulated *S. europaea* PM proteins identified by MALDI-TOF/TOF.

Table S4. Protein distribution in the eight clusters.

Table S5. Specific primers used for real-time PCR of genes encoding calcium signalling components of *S. europaea*.

Acknowledgements

This work was supported by the Research Programs from the Chinese Ministry of Agriculture (grant no. 2014ZX08009-003-002), the National Natural Science Foundation of China (grant no. 31200201), and the Science and Technology Service Network Initiative of the Chinese Academy of Sciences (grant no. KFJ-EW-STS-061-4). The authors thank Dafeng Jinglong Marine Industrialized Development Corporation, Ltd, Jiangsu Province for providing seeds of *S. europaea*. All authors have declared no conflict of interest.

References

Aghaei K, Ehsanpour AA, Komatsu S. 2008. Proteome analysis of potato under salt stress. *Journal of Proteome Research* **7,** 4858–4868.

Bar Y, Apelbaum A, Kafkafi U, Goren R. 1997. Relationship between chloride and nitrate and its effect on growth and mineral composition of avocado and citrus plants. *Journal of Plant Nutrition* **20,** 715–731.

Cheng Y, Qi Y, Zhu Q, Chen X, Wang N, Zhao X, Chen H, Cui X, Xu L, Zhang W. 2009. New changes in the plasma-membrane-associated proteome of rice roots under salt stress. *Proteomics* **9,** 3100–3114.

Davies JM. 2014. Annexin-mediated calcium signalling in plants. *Plants* **3,** 128–140.

Debouba M, Dguimi HM, Ghorbel M, Gouia H, Suzuki A. 2013. Expression pattern of genes encoding nitrate and ammonium assimilating enzymes in *Arabidopsis thaliana* exposed to short term NaCl stress. *Journal of Plant Physiology* **170,** 155–160.

DeFalco TA, Bender KW, Snedden WA. 2010. Breaking the code: Ca^{2+} sensors in plant signalling. *Biochemical Journal* **425,** 27–40.

D'Onofrio C, Lindberg S. 2009. Sodium induces simultaneous changes in cytosolic calcium and pH in salt-tolerant quince protoplasts. *Journal of Plant Physiology* **166,** 1755–1763.

Elmore JM, Liu J, Smith B, Phinney B, Coaker G. 2012. Quantitative proteomics reveals dynamic changes in the plasma membrane during *Arabidopsis* immune signaling. *Molecular and Cellular Proteomics* **11,** M111.014555.

Fan PX, Nie LL, Jiang P, Feng JJ, Lv SL, Chen XY, Bao HXG, Guo J, Tai F, Wang JH. 2013. Transcriptome analysis of *Salicornia europaea* under saline conditions revealed the adaptive primary metabolic pathways as early events to facilitate salt adaptation. *PLoS One* **8,** e80595.

Flowers TJ, Colmer TD. 2008. Salinity tolerance in halophytes. *New Phytologist* **179,** 945–963.

Frechilla S, Lasa B, Ibarretxe L, Lamsfus C, Aparicio-Tejo P. 2001. Pea responses to saline stress is affected by the source of nitrogen nutrition (ammonium or nitrate). *Plant Growth Regulation* **35,** 171–179.

Guo C, Chang W, Gu J, Li X, Lu W, Xiao K. 2011. Molecular characterization, transcriptional regulation and function analysis of nitrate transporters in plants. *Frontiers of Agriculture in China* **5,** 291–298.

Halperin SJ, Gilroy S, Lynch JP. 2003. Sodium chloride reduces growth and cytosolic calcium, but does not affect cytosolic pH, in root hairs of *Arabidopsis thaliana* L. *Journal of Experimental Botany* **54,** 1269–1280.

Hamed KB, Ellouzi H, Talbi OZ, Hessini K, Slama I, Ghnaya T, Bosch SM, Savouré A, Abdelly C. 2013. Physiological response of halophytes to multiple stresses. *Functional Plant Biology* **40,** 883–896.

Ho CH, Lin SH, Hu HC, Tsay YF. 2009. CHL1 functions as a nitrate sensor in plants. *Cell* **138,** 1184–1194.

Hu HC, Wang YY, Tsay YF. 2009. AtCIPK8, a CBL-interacting protein kinase, regulates the low-affinity phase of the primary nitrate response. *The Plant Journal* **57,** 264–278.

Jampeetong A, Brix H. 2009. Nitrogen nutrition of *Salvinia natans*: effects of inorganic nitrogen form on growth, morphology, nitrate reductase activity and uptake kinetics of ammonium and nitrate. *Aquatic Botany* **90,** 67–73.

Jia XY, He LH, Jing RL, Li RZ. 2009. Calreticulin: conserved protein and diverse functions in plants. *Physiologia Plantarum* **136,** 127–138.

Jiang Y, Yang B, Harris NS, Deyholos MK. 2007. Comparative proteomic analysis of NaCl stress-responsive proteins in *Arabidopsis* roots. *Journal of Experimental Botany* **58,** 3591–3607.

Kader MA, Lindberg S. 2010. Cytosolic calcium and pH signaling in plants under salinity stress. *Plant Signaling and Behavior* **5,** 233–238.

Kader MA, Lindberg S, Seidel T, Golldack D, Yemelyanov V. 2007. Sodium sensing induces different changes in free cytosolic calcium concentration and pH in salt-tolerant and -sensitive rice (*Oryza sativa*) cultivars. *Physiologia Plantarum* **130,** 99–111.

Krapp A, David LC, Chardin C, Girin T, Marmagne A, Leprince A-S, Chaillou S, Ferrario-Méry S, Meyer C, Daniel-Vedele F. 2014. Nitrate transport and signalling in *Arabidopsis*. *Journal of Experimental Botany* **65,** 789–798.

Kudla J, Batistic O, Hashimoto K. 2010. Calcium signals: the lead currency of plant information processing. *The Plant Cell* **22,** 541–563.

Lambeck I, Chi JC, Krizowski S, Mueller S, Mehlmer N, Teige M, Fischer K, Schwarz G. 2010. Kinetic analysis of 14-3-3-inhibited *Arabidopsis thaliana* nitrate reductase. *Biochemistry* **49,** 8177–8186.

Lara C, Rodríguez R, Guerrero MG. 1993. Sodium dependent nitrate transport and energetics in cyanobacteria. *Journal of Phycology* **29,** 389–395.

Latz A, Mehlmer N, Zapf S, Mueller TD, Wurzinger B, Pfister B, Csaszar E, Hedrich R, Teige M, Becker D. 2013. Salt stress triggers phosphorylation of the *Arabidopsis* vacuolar K^+ channel TPK1 by calcium-dependent protein kinases (CDPKs). *Molecular Plant* **6,** 1274–1289.

Liu CW, Chang TS, Hsu YK, Wang AZ, Yen HC, Wu YP, Wang CS, Lai CC. 2014. Comparative proteomic analysis of early salt stress responsive proteins in roots and leaves of rice. *Proteomics* **14,** 1759–1775.

Lv SL, Jiang P, Chen XY, Fan PX, Wang XC, Li YX. 2012. Multiple compartmentalization of sodium conferred salt tolerance in *Salicornia europaea*. *Plant Physiology and Biochemistry* **51,** 47–52.

Lynch J, Läuchli A. 1988. Salinity affects intracellular calcium in corn root protoplasts. *Plant Physiology* **87,** 351–356.

Ma J, Zhang M, Xiao X, You J, Wang J, Wang T, Yao Y, Tian C. 2013. Global transcriptome profiling of *Salicornia europaea* L. shoots under NaCl treatment. *PLoS One* **8,** e65877.

Magnan F, Ranty B, Charpenteau M, Sotta B, Galaud JP, Aldon D. 2008. Mutations in AtCML9, a calmodulin-like protein from *Arabidopsis thaliana*, alter plant responses to abiotic stress and abscisic acid. *The Plant Journal* **56,** 575–589.

Mansour M. 2000. Nitrogen containing compounds and adaptation of plants to salinity stress. *Biologia Plantarum* **43,** 491–500.

Marschner H, Rimmington G. 1988. Mineral nutrition of higher plants. *Plant, Cell and Environment* **11,** 147–148.

Masclaux-Daubresse C, Daniel-Vedele F, Dechorgnat J, Chardon F, Gaufichon L, Suzuki A. 2010. Nitrogen uptake, assimilation and remobilization in plants: challenges for sustainable and productive agriculture. *Annals of Botany* **105,** 1141–1157.

Mehlmer N, Wurzinger B, Stael S, Hofmann-Rodrigues D, Csaszar E, Pfister B, Bayer R, Teige M. 2010. The Ca^{2+}-dependent protein kinase CPK3 is required for MAPK-independent salt-stress acclimation in *Arabidopsis*. *The Plant Journal* **63,** 484–498.

Moller AL, Pedas P, Andersen B, Svensson B, Schjoerring JK, Finnie C. 2011. Responses of barley root and shoot proteomes to long-term nitrogen deficiency, short-term nitrogen starvation and ammonium. *Plant, Cell and Environment* **34,** 2024–2037.

Munns R, Tester M. 2008. Mechanisms of salinity tolerance. *Annual Review of Plant Biology* **59,** 651–681.

Muños S, Cazettes C, Fizames C, Gaymard F, Tillard P, Lepetit M, Lejay L, Gojon A. 2004. Transcript profiling in the *chl1-5* mutant of *Arabidopsis* reveals a role of the nitrate transporter NRT1.1 in the regulation of another nitrate transporter, NRT2.1. *The Plant Cell* **16,** 2433–2447.

Nie LL, Feng JJ, Lv SL, Jiang P, Fan PX, Tai F, Li YX. 2012. The response of euhalophyte *Salicornia europaea* L. to different nitrogen forms. *Acta Ecologica Sinica* **32,** 5703–5712.

Nouri MZ, Komatsu S. 2010. Comparative analysis of soybean plasma membrane proteins under osmotic stress using gel-based and LC MS/MS-based proteomics approaches. *Proteomics* **10,** 1930–1945.

Pauly B, Lasi M, MacKintosh C, Morrice N, Imhof A, Regula J, Rudd S, David CN, Bottger A. 2007. Proteomic screen in the simple metazoan Hydra identifies 14-3-3 binding proteins implicated in cellular metabolism, cytoskeletal organisation and Ca^{2+} signalling. *BMC Cell Biology* **8,** 31.

Pessarakli M, Harivandi M, Kopec DM, Ray DT. 2012. Growth responses and nitrogen uptake by saltgrass (*Distichlis spicata* L.), a halophytic plant species, under salt stress, using the ^{15}N technique. *International Journal of Agronomy* **2012,** 896971.

Plieth C. 2005. Calcium: just another regulator in the machinery of life? *Annals of Botany* **96,** 1–8.

Popescu SC, Popescu GV, Bachan S, Zhang Z, Seay M, Gerstein M, Snyder M, Dinesh-Kumar S. 2007. Differential binding of calmodulin-related proteins to their targets revealed through high-density *Arabidopsis* protein microarrays. *Proceedings of the National Academy of Sciences, USA* **104,** 4730–4735.

Prinsi B, Negri AS, Pesaresi P, Cocucci M, Espen L. 2009. Evaluation of protein pattern changes in roots and leaves of *Zea mays* plants in response to nitrate availability by two-dimensional gel electrophoresis analysis. *BMC Plant Biology* **9,** 113.

Rees TAV, Cresswell RC, Syrett PJ. 1980. Sodium-dependent uptake of nitrate and urea by a marine diatom. *Biochimica et Biophysica Acta* **596,** 141–144.

Rubio L, Linares-Rueda A, García-Sánchez M, Fernández J. 2005. Physiological evidence for a sodium-dependent high-affinity phosphate and nitrate transport at the plasma membrane of leaf and root cells of *Zostera marina* L. *Journal of Experimental Botany* **56,** 613–622.

Striker GG, Teakle NL, Colmer TD, Barrett-Lennard ED. 2015. Growth responses of *Melilotus siculus* accessions to combined salinity and root-zone hypoxia are correlated with differences in tissue ion concentrations and not differences in root aeration. *Environmental and Experimental Botany* **109,** 89–98.

Tang W. 2012. Quantitative analysis of plasma membrane proteome using two-dimensional difference gel electrophoresis. *Methods in Molecular Biology* **876,** 67–82.

Tang W, Kim TW, Oses-Prieto JA, Sun Y, Deng Z, Zhu S, Wang R, Burlingame AL, Wang ZY. 2008. BSKs mediate signal transduction from the receptor kinase BRI1 in *Arabidopsis*. *Science* **321,** 557–560.

Taylor NL, Heazlewood JL, Millar AH. 2011. The *Arabidopsis thaliana* 2-D gel mitochondrial proteome: refining the value of reference maps for assessing protein abundance, contaminants and post-translational modifications. *Proteomics* **11,** 1720–1733.

Ungar IA. 1987. Population characteristics, growth and survival of the halophyte *Salicornia europaea*. *Ecology* **68,** 569–575.

Vialaret J, Di Pietro M, Hem S, Maurel C, Rossignol M, Santoni V. 2014. Phosphorylation dynamics of membrane proteins from *Arabidopsis* roots submitted to salt stress. *Proteomics* **14,** 1058–1070.

Vidal EA, Tamayo KP, Gutierrez RA. 2010. Gene networks for nitrogen sensing, signaling, and response in *Arabidopsis thaliana*. *Wiley Interdisciplinary Reviews: Systems Biology and Medicine* **2,** 683–693.

Wang X, Bian YY, Cheng K, Zou HF, Sun SSM, He JX. 2012. A comprehensive differential proteomic study of nitrate deprivation in *Arabidopsis* reveals complex regulatory networks of plant nitrogen responses. *Journal of Proteome Research* **11,** 2301–2315.

Wang XC, Li XF, Deng X, Han HP, Shi WL, Li YX. 2007. A protein extraction method compatible with proteomic analysis for the euhalophyte *Salicornia europaea*. *Electrophoresis* **28,** 3976–3987.

Wang XC, Fan PX, Song HM, Chen XY, Li XF, Li YX. 2009. Comparative proteomic analysis of differentially expressed proteins in shoots of *Salicornia europaea* under different salinity. *Journal of Proteome Research* **8,** 3331–3345.

Wessel D, Flügge UI. 1984. A method for the quantitative recovery of protein in dilute solution in the presence of detergents and lipids. *Analytical Biochemistry* **138,** 141–143.

Wu D, Shen Q, Qiu L, Han Y, Ye L, Jabeen Z, Shu Q, Zhang G. 2014. Identification of proteins associated with ion homeostasis and salt tolerance in barley. *Proteomics* **14,** 1381–1392.

Yaneva IA, Hoffmann GW, Tischner R. 2002. Nitrate reductase from winter wheat leaves is activated at low temperature via protein dephosphorylation. *Physiologia Plantarum* **114,** 65–72.

Yuan JF, Tian CY, Feng G. 2010. Effects of sodium on nitrate uptake and osmotic adjustment of *Suaeda physophora*. *Journal of Arid Land* **2,** 190–196.

Zhang Y, Ding S, Lu Q, Yang Z, Wen X, Zhang L, Lu C. 2011. Characterization of photosystem II in transgenic tobacco plants with decreased iron superoxide dismutase. *Biochimica et Biophysica Acta* **1807,** 391–403.